

- not to carnivore mass ($F = 26.94$; $df = 2, 22$; $P < 0.0001$; prey biomass: $F = 6.42$, $P < 0.016$; body mass: $F = 0.26$, not significant). Controlling for phylogeny (23, 24), we get a similar result: $\ln(\text{number per } 10,000 \text{ kg of prey}) + 1 = -1.12 \times \ln(\text{carnivore mass})$; $r = 0.753$, $P < 0.01$. One contrast in the body mass and prey biomass analysis was excluded, calculated between *Lynx* and *Panthera*, because it had a Studentized deleted residual greater than 3.
23. A. Purvis, A. Rambaut, *Comput. Appl. Biosci.* **11**, 247 (1995).
 24. O. R. P. Bininda-Emonds, J. L. Gittleman, A. Purvis, *Biol. Rev.* **74**, 143 (1999).
 25. K. S. Smallwood, C. Schonewald, *Oecologia* **105**, 329 (1996).
 26. T. M. Blackburn, K. J. Gaston, *Oikos* **75**, 303 (1996).
 27. T. K. Fuller, D. L. Murray, *Anim. Conserv.* **1**, 153 (1998).
 28. Controlling for phylogeny yields the following expression: $\ln(\text{number per productivity}) = -0.36 \times \ln(\text{carnivore mass})$; $r = 0.449$, $P < 0.05$. The contrast between canids and felids had a large leverage and was removed.
 29. T. K. Fuller, P. R. Sievert, in *Carnivore Conservation*, J. L. Gittleman, S. M. Funk, D. W. Macdonald, R. K. Wayne, Eds. (Cambridge Univ. Press, Cambridge, 2001), pp. 163–178.
 30. M. G. L. Mills, M. L. Gorman, *Conserv. Biol.* **11**, 1397 (1997).
 31. K. M. Laursen, N. Wielebnowski, T. M. Caro, *Conserv. Biol.* **9**, 1329 (1995).
 32. W. A. Calder, in *Scaling in Biology: Patterns, Processes, Causes and Consequences*, J. H. Brown, G. B. West, Eds. (Oxford Univ. Press, Oxford, 2000), pp. 297–323.
 33. K. J. Gaston, T. M. Blackburn, *Patterns and Processes in Macroecology* (Blackwell Scientific, Oxford, 2000).
 34. S. P. Hubbell, *The Unified Neutral Theory of Biodiversity and Biogeography* (Princeton Univ. Press, Princeton, NJ, 2001).
 35. A. Molinari-Jobin, P. Molinari, C. Breitenmoser-Würsten, U. Breitenmoser, *Wildlife Biol.*, in press.
 36. A. Jobin, P. Molinari, U. Breitenmoser, *Acta Theriol.* **45**, 243 (2000).
 37. B. Jedrzejewski, W. Jedrzejewski, *Predation in Vertebrate Communities: The Białowieża Primeval Forest as a Case Study* (Springer-Verlag, Berlin, 1998).

38. A. F. Vezina, *Oecologia* **67**, 555 (1985).
39. J. L. Gittleman, M. E. Gompper, *Science* **291**, 997 (2001).
40. J. Berger, J. E. Swanson, I. L. Persson, *Science* **291**, 1036 (2001).
41. C. Hilton-Taylor (Compiler), *2000 IUCN Red List of Threatened Species* (IUCN–The World Conservation Union, Gland, Switzerland, 2000).
42. A. Purvis, J. L. Gittleman, G. Cowlshaw, G. M. Mace, *Proc. R. Soc. London Ser. B* **267**, 1947 (2000).
43. A version of the table with a full list of references can be found at *Science Online* at www.sciencemag.org/cgi/content/full/295/5563/2273/DC1.
44. We thank K. Gaston, J. Brown, K. Jones, P. Bennett, S. Funk, M. Rowcliffe, C. Mueller, A. Bourke, G. Mace, T. Coulson, S. Semple, J. Du Toit, J. Fulford, I. J. Gordon, and three anonymous referees for helpful discussions and comments on earlier drafts of the manuscript. We are grateful to the following for access to data: A. Jobin, Z. T. Ashenafi, K. Murphy, S. Roy, A. Venkataraman, A. T. Johnsingh, A. Angebjorn, and T. Coonan.

13 November 2001; accepted 21 January 2002

Neuronal Calcium Sensor 1 and Activity-Dependent Facilitation of P/Q-Type Calcium Currents at Presynaptic Nerve Terminals

Tetsuhiro Tsujimoto,^{1*†} Andreas Jeromin,^{2*} Naoto Saitoh,¹ John C. Roder,² Tomoyuki Takahashi¹

P/Q-type presynaptic calcium currents (I_{pCa}) undergo activity-dependent facilitation during repetitive activation at the calyx of the Held synapse. We investigated whether neuronal calcium sensor 1 (NCS-1) may underlie this phenomenon. Direct loading of NCS-1 into the nerve terminal mimicked activity-dependent I_{pCa} facilitation by accelerating the activation time of I_{pCa} in a Ca^{2+} -dependent manner. A presynaptically loaded carboxyl-terminal peptide of NCS-1 abolished I_{pCa} facilitation. These results suggest that residual Ca^{2+} activates endogenous NCS-1, thereby facilitating I_{pCa} . Because both P/Q-type Ca^{2+} channels and NCS-1 are widely expressed in mammalian nerve terminals, NCS-1 may contribute to the activity-dependent synaptic facilitation at many synapses.

Neurotransmitter release is triggered by Ca^{2+} influx through presynaptic voltage-dependent Ca^{2+} channels (I). Modulation in the presynaptic calcium current (I_{pCa}) results in robust alteration of synaptic efficacy because of their nonlinear relationship (2). At the calyx of Held nerve terminal, repetitive activation of Ca^{2+} channels increases the amplitudes of I_{pCa} (3–5). The magnitude of I_{pCa} facilitation is dependent on the extracellular Ca^{2+} concentration and is attenuated by intraterminal loading of Ca^{2+} chelating agents (4, 5). This

I_{pCa} facilitation is distinct from the voltage-dependent relief of Ca^{2+} channels from tonic inhibition by heterotrimeric guanine nucleotide binding (G) proteins (6, 7), because presynaptic loadings of guanine nucleotide analogs have no effect (4). A Ca^{2+} -binding protein may thus be involved in the activity-dependent I_{pCa} facilitation.

Among neuron-specific Ca^{2+} -binding proteins, frequenin was first cloned from *Drosophila T(X;Y) V7* mutants (8). Later, the frequenin homolog NCS-1 was cloned from a variety of species (9–14). NCS-1 (frequenin) is widely expressed in neuronal somata, dendrites, and nerve terminals (14–18) throughout embryonic and postnatal development (14, 17). Overexpression (19) or intracellular loading of NCS-1 in motoneurons (10) enhances neuromuscular transmission. We investigated whether NCS-1 is involved in the

activity-dependent I_{pCa} facilitation at the calyx of Held synapse.

Whole-cell voltage-clamp recordings were made from a calyceal nerve terminal (20), and I_{pCa} was elicited by an action potential waveform command pulse at 0.1 Hz. The half-width and the peak amplitude of a prerecorded action potential were similar to those reported for afferent fiber-stimulated action potentials in 14-day-old rats (21). After a stable epoch of I_{pCa} , NCS-1 was infused into a nerve terminal through a perfusion tube (Fig. 1A). After infusion, amplitudes of I_{pCa} gradually increased, reached a maximum in 5 min, and then gradually declined. This decline may be caused by “adaptation” in the mechanism of facilitation by NCS-1, because I_{pCa} elicited at 0.1 Hz does not undergo run-down for more than 20 min (22). The mean magnitude of I_{pCa} facilitation 5 min after the onset of NCS-1 infusion was $113 \pm 37\%$ (mean \pm SEM, $n = 3$).

We next examined the effect of NCS-1 on I_{pCa} elicited by a 5-ms depolarizing pulse. When NCS-1 was included in the presynaptic pipette solution, the rise time of I_{pCa} was significantly faster than rise times in the presence of heat-inactivated (H.I.) NCS-1 or in the absence of NCS-1 [Fig. 1, B (inset) and C]. The current-voltage (I - V) relationship of I_{pCa} measured at 1 ms after the onset of the command pulse had a peak at -10 mV in the presence of NCS-1, whereas the peaks were at 0 mV in the presence of H.I. NCS-1 or in the absence of NCS-1 (Fig. 1B). Similarly, in the presence of NCS-1, the half-activation voltage ($V_{1/2}$) calculated from the modified Boltzmann equation (20) was significantly more negative than those in the presence of H.I. NCS-1 or in the absence of NCS-1 (Fig. 1D). However, NCS-1 had no effect on the magnitude of plateau Ca^{2+} currents (Fig. 1E).

NCS-1 has four helix-to-helix Ca^{2+} -binding architectures (EF-hands) and binds three

¹Department of Neurophysiology, University of Tokyo Faculty of Medicine, Tokyo 113-0033, Japan.
²Mount Sinai Hospital Research Institute, Toronto, Ontario M5G 1X5, Canada.

*These authors contributed equally to this work.

†To whom correspondence should be addressed. E-mail: tujimoto-ty@umin.ac.jp

Ca²⁺ ions (12). To examine whether the facilitatory effect of NCS-1 on I_{pCa} is Ca²⁺-dependent, we loaded the Ca²⁺ chelator 1,2-bis(*o*-aminophenoxy)ethane-*N,N,N',N'*-tetraacetic acid (BAPTA) into calyces together with NCS-1. In the presence of BAPTA, NCS-1 no longer shortened the rise time of I_{pCa} (Fig. 1C), nor did it cause the negative shift in $V_{1/2}$ (Fig. 1, B and D).

The effect of NCS-1 on I_{pCa} mimics the activity-dependent facilitation induced by repetitive stimulation (3–5) with respect to (i) the shortened rise time of I_{pCa} , (ii) the negative shift in $V_{1/2}$, and (iii) its Ca²⁺ dependency. To further examine whether the NCS-1-induced fa-

cilitation and the activity-dependent facilitation of I_{pCa} share a common mechanism, we carried out an occlusion experiment. When NCS-1 was included in the presynaptic pipette, the magnitude of I_{pCa} facilitation induced by a pair of brief depolarizations was significantly smaller than those in the presence of heat-inactivated NCS-1 or in the absence of NCS-1 (Fig. 2); these findings indicate that NCS-1 partially occluded the activity-dependent I_{pCa} facilitation.

Although mRNAs encoding NCS-1 are expressed in the rodent brainstem (14, 18), it is not known whether NCS-1 is expressed at this terminal. Immunocytochemical examinations using antibody to NCS-1 (20) revealed NCS-1

immunoreactivity both in the medial nucleus of the trapezoid body (MNTB) cell somata and in the calyceal terminal, the latter being colocalized with the immunoreactivity of the presynaptic marker syntaxin (Fig. 3A). The specificity of the NCS-1 immunofluorescence was confirmed by absorption experiments (Fig. 3B). The immunocytochemical resolution distinguishing the pre- and postsynaptic signals was confirmed by a separation in the signal of the postsynaptic cell body marker microtubule-associated protein 2B (MAP2B) from that of syntaxin (Fig. 3C).

A unique feature of NCS-1 is the large conformational shift of its COOH-terminal region, creating a wide hydrophobic crevice for the target recognition (13). Thus, a COOH-terminal fragment peptide (20) might inhibit the interactions between NCS-1 and P/Q-type Ca²⁺ channels. When the COOH-terminal peptide was loaded into the calyces, the facilitation of I_{pCa} elicited by a paired-pulse protocol was abolished ($P < 0.001$), whereas the scrambled peptide (20) had no such effect (Fig. 4A). The COOH-terminal peptide loaded into calyces had no appreciable effect on I_{pCa} with respect to current kinetics or I - V relationships (Fig. 4B). The COOH-terminal peptide also blocked the I_{pCa}

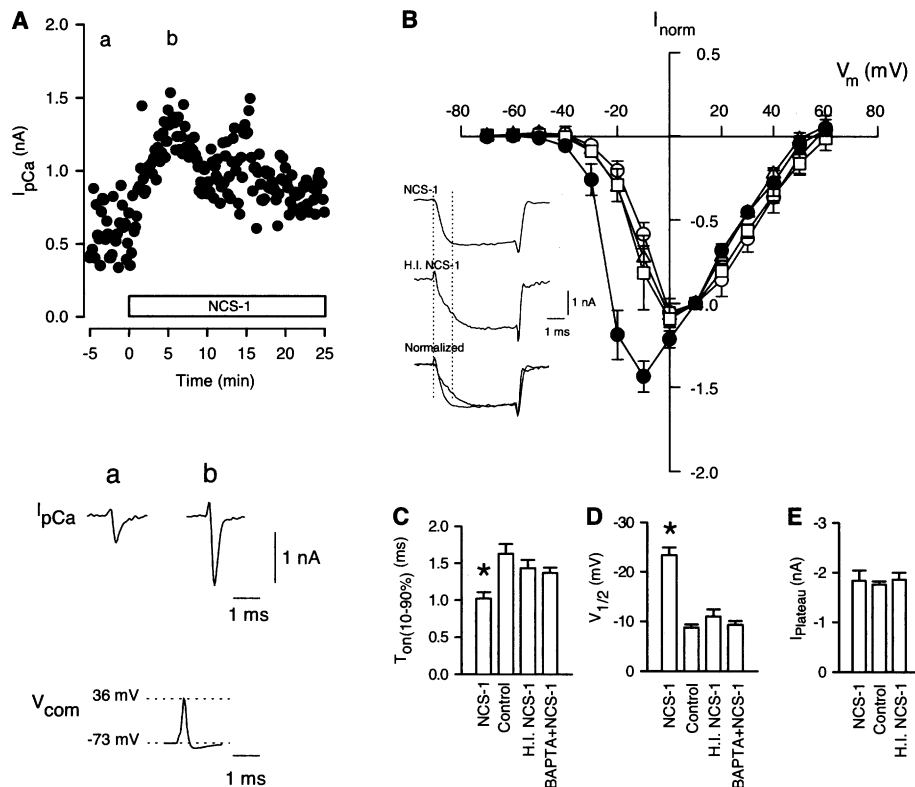


Fig. 1. Facilitation of I_{pCa} by NCS-1. **(A)** After stable I_{pCa} recordings, NCS-1 (200 μ M) was injected into the nerve terminal via pipette perfusion during the period indicated by a bar. Because of the large molecular weight of NCS-1 (20 kD) and the distance between the tips of the perfusion tube and the pipette, final concentration in the calyx could not be assessed. Sample traces below the plot are six averaged I_{pCa} measurements before (a) and 5 min after the infusion (b). An action potential waveform used for the command pulse (V_{com}) was obtained from another calyceal terminal by means of an intracellular recording amplifier. The spike was evoked by injecting a brief depolarizing current pulse (0.12 ms). The action potential had an overshoot of 36 mV and half-width of 0.20 ms. **(B)** The I - V relationships of I_{pCa} measured at 1 ms after the depolarizing pulse onset, normalized to the current amplitudes at +10 mV. Symbols: \circ , control (no NCS-1); \bullet , NCS-1 (10 μ M); \square , heat-inactivated (H.I.) NCS-1 (10 μ M); \triangle , NCS-1 plus BAPTA (16 mM). The peak of the I - V relationship in the presence of NCS-1 shows the negative shift compared with the others. Inset: In three calyces under voltage-clamp, I_{pCa} was elicited by a depolarizing command pulse (5 ms) from a holding potential (-80 mV) to -10 mV every 10 s. Vertical dotted lines indicate the pulse onset and 1 ms after the onset. I_{pCa} traces in the presence of NCS-1 (top) or H.I. NCS-1 (middle) are normalized in peak amplitude and superimposed for comparison (bottom). **(C)** The 10 to 90% rise time of I_{pCa} in the presence of NCS-1 (1.02 ± 0.09 ms, $n = 5$) is significantly faster ($*P < 0.01$, analysis of variance) than in the control (1.63 ± 0.13 ms, $n = 6$), H.I. NCS-1 (1.43 ± 0.11 ms, $n = 6$), and BAPTA + NCS-1 (1.37 ± 0.07 ms, $n = 3$) conditions. **(D)** $V_{1/2}$ of I_{pCa} in the presence of NCS-1 (-23.4 ± 1.5 mV, $n = 4$) was more negative ($*P < 0.001$) than in the control (-8.7 ± 0.7 mV, $n = 5$), H.I. NCS-1 (-11.0 ± 1.4 mV, $n = 4$), and BAPTA + NCS-1 (-9.3 ± 0.8 mV, $n = 3$) conditions. **(E)** In the presence of NCS-1, H.I. NCS-1, or no NCS-1, the peak amplitudes of I_{pCa} measured at 5 ms from the command pulse onset are similar ($P > 0.5$).

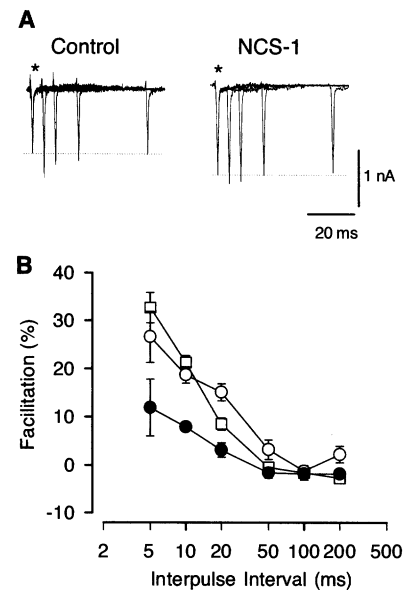


Fig. 2. Occlusion of activity-dependent I_{pCa} facilitation by NCS-1. **(A)** In a paired-pulse protocol, I_{pCa} was evoked every 10 s by a pair of 1-ms square-wave command pulses to -10 mV at interpulse intervals of 5, 10, 20, and 50 ms (superimposed). Left, a calyx in the absence of NCS-1 (control); right, another calyx in the presence of NCS-1. Horizontal dotted lines indicate the amplitudes of the first I_{pCa} (*) in the paired-pulse protocol. **(B)** Summarized data of paired-pulse facilitation at various interpulse intervals in the presence of NCS-1 ($n = 5$, \bullet), H.I. NCS-1 ($n = 7$, \square), and no NCS-1 ($n = 5$, \circ). Error bars are merged into some data points.

REPORTS

facilitation induced by a 100-Hz train (Fig. 4C). Because the COOH-terminal peptide lacks the flanking sequence required for efficient Ca^{2+} binding, it cannot work by reducing the Ca^{2+} concentration in calyces. Thus, the COOH-terminal fragment of NCS-1 is likely to interfere with the interaction between NCS-1 and P/Q-type Ca^{2+} channels, thereby blocking the activity-dependent I_{pCa} facilitation.

The Ca^{2+} channel subtype expressed at the calyceal terminal of rats used in this study (14 to 18 days old) is purely P/Q-type (3, 23). The presynaptic P/Q-type Ca^{2+} currents have a single fast activation phase (<2 ms), which can be shortened by a conditioning depolarization (4) or presynaptic loading of NCS-1 (Fig. 1, B and C). In contrast, currents of recombinant P/Q-type Ca^{2+} channels expressed in human embryonic kidney-293 cells show a slow activation phase (>10 ms) after a fast activation phase (24). A conditioning depolarization makes this slow activation phase merge into the fast one, and this effect has been attributed to

calmodulin (24). At the calyx of Held, however, a calmodulin inhibitory peptide has no effect on I_{pCa} (25). Thus, calmodulin does not likely play a role in the I_{pCa} facilitation, at least at this synapse. NCS-1 mediates the facilitatory effect of glial cell line-derived neurotrophic factor (GDNF) on N-type Ca^{2+} currents in motoneurons and on transmitter release at the neuromuscular junction (26). This phenomenon is also distinct from the activity-dependent I_{pCa} facilitation, because GDNF increases the peak amplitude of N-type Ca^{2+} currents without affecting their activation kinetics.

At the calyx of Held nerve terminal, overall Ca^{2+} concentration increases to $0.4 \mu\text{M}$ in response to a single action potential (27). NCS-1 can bind three Ca^{2+} ions with an affinity of $10 \mu\text{M}$ (second EF-hand) and $0.4 \mu\text{M}$ (third and fourth EF-hands) (12). Thus, residual Ca^{2+} after an action potential may bind with NCS-1, thereby accelerating the activation time of P/Q-type Ca^{2+} channels.

In mammals, synaptic transmission is largely mediated by P/Q-type Ca^{2+} currents

both in the peripheral (28) and central (29) nervous system, and their contribution to transmitter release increases with postnatal

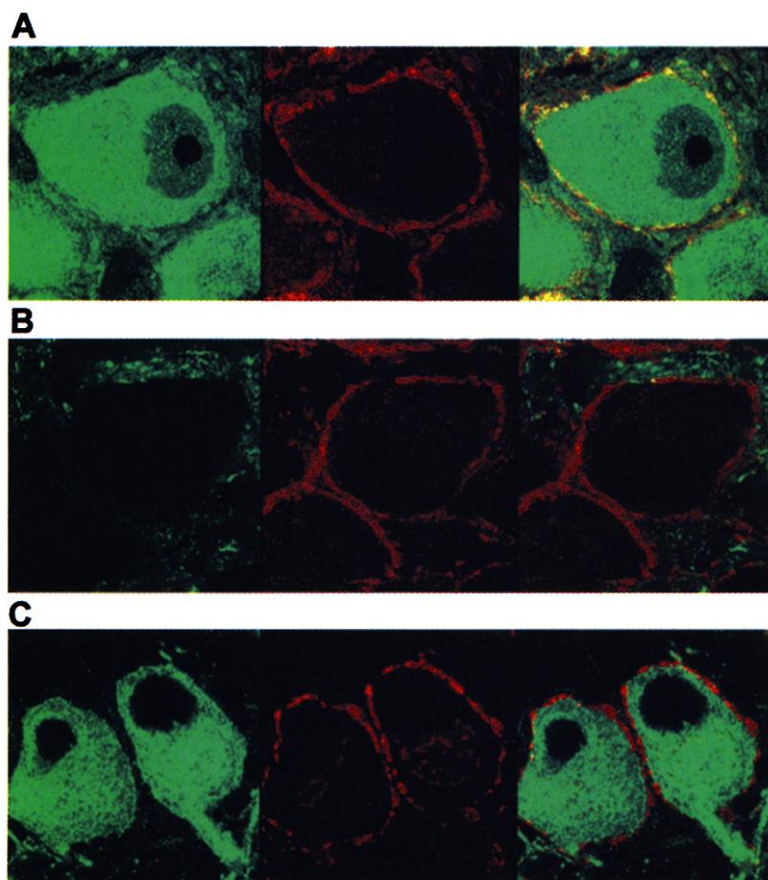


Fig. 3. NCS-1 immunoreactivity at calyceal nerve terminals. (A) NCS-1 immunofluorescence signal (green, left) and syntaxin immunofluorescence signal (red, center) partially overlapped (yellow, right), indicating that NCS-1 is expressed in both the presynaptic and postsynaptic compartments. (B) Pretreatment of antibody to NCS-1 with exogenous NCS-1. No clear NCS-1 immunofluorescence signal was observed, whereas the syntaxin signal remained unchanged. (C) Immunofluorescence signal for MAP2B (green, left) and syntaxin signal (red, center) showed no overlap when superimposed (right). Scale bar, $10 \mu\text{m}$.

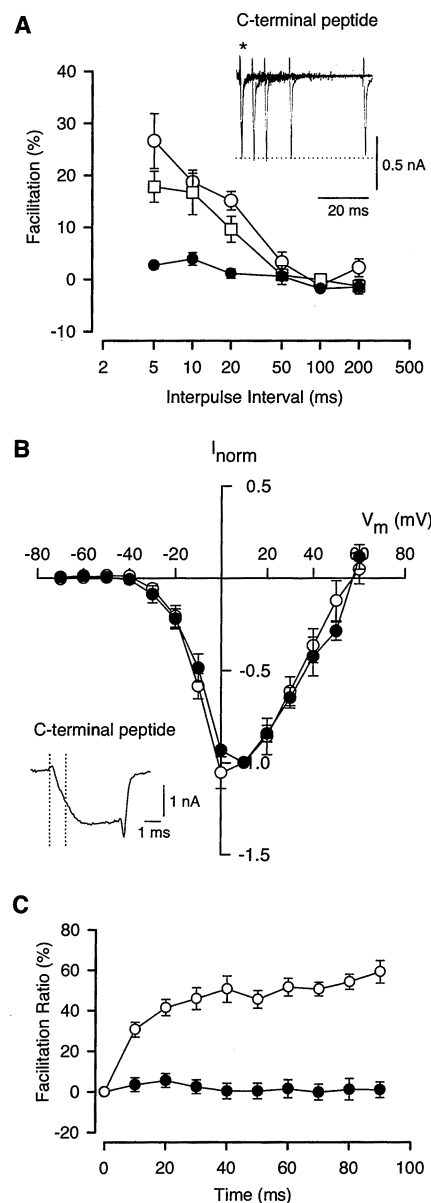


Fig. 4. COOH-terminal fragment peptide of NCS-1 inhibits the activity-dependent I_{pCa} facilitation. (A) The facilitation ratio at various intervals in the presence of the COOH-terminal peptide ($50 \mu\text{M}$, $n = 6$, ●, sample traces in inset), scrambled peptide ($50 \mu\text{M}$, $n = 3$, □), or no peptide ($n = 5$, ○). (B) The I - V relationships of I_{pCa} in the presence of the COOH-terminal peptide ($V_{1/2} = -6.5 \pm 0.7 \text{ mV}$, $n = 3$, ●, $P = 0.08$, sample trace in inset) or no peptide ($V_{1/2} = -8.7 \pm 0.7 \text{ mV}$, $n = 5$, ○). In the presence of scrambled peptide, $V_{1/2}$ was similar (-6.8 mV , $n = 2$, not shown). (C) Mean magnitude of I_{pCa} facilitation during a train of short depolarizing pulses (to -10 mV , 1 ms , 10 ms interval). COOH-terminal peptide abolished the I_{pCa} facilitation induced by a tetanic stimulation (100 Hz) every 20 s. Ten consecutive data points in control (○, $n = 4$) and in the presence of the COOH-terminal peptide (●, $n = 3$) are shown.

development (30). Given the wide distribution of NCS-1 in the nerve terminals (14–18), the activity-dependent I_{pCa} facilitation may be mediated by NCS-1 at various synapses, thereby mediating activity-dependent synaptic facilitation. The residual Ca^{2+} hypothesis for the synaptic facilitation has been widely accepted, but its detailed mechanism is still unknown (31). One of the downstream effects of residual Ca^{2+} is the facilitation of I_{pCa} (3–5). Hence, our results suggest that NCS-1 may be a key molecule for the activity-dependent synaptic facilitation.

References and Notes

1. B. Katz, R. Miledi, *J. Physiol.* **189**, 535 (1967).
2. F. A. Dodge Jr., R. Rahamimoff, *J. Physiol.* **193**, 419 (1967).
3. I. D. Forsythe, T. Tsujimoto, M. Barnes-Davies, M. F. Cuttle, T. Takahashi, *Neuron* **20**, 797 (1998).
4. M. F. Cuttle, T. Tsujimoto, I. D. Forsythe, T. Takahashi, *J. Physiol.* **512**, 723 (1998).
5. J. G. G. Borst, B. Sakmann, *J. Physiol.* **513**, 149 (1998).

6. S. R. Ikeda, *J. Physiol.* **439**, 181 (1991).
7. H. Kasai, *J. Physiol.* **448**, 189 (1992).
8. O. Pongs et al., *Neuron* **11**, 15 (1993).
9. S. Nef, H. Fiumelli, E. De Castro, M. B. Raes, P. Nef, *J. Recept. Signal Transduct. Res.* **15**, 365 (1995).
10. P. Olafsson, T. Wang, B. Lu, *Proc. Natl. Acad. Sci. U.S.A.* **92**, 8001 (1995).
11. E. De Castro et al., *Biochem. Biophys. Res. Commun.* **216**, 133 (1995).
12. J. B. Ames et al., *Biochemistry* **39**, 12149 (2000).
13. Y. Bourne, J. Dannenberg, V. Pollmann, P. Marchot, O. Pongs, *J. Biol. Chem.* **276**, 11949 (2001).
14. P. Olafsson et al., *Mol. Brain Res.* **44**, 73 (1997).
15. N. C. Schaad et al., *Proc. Natl. Acad. Sci. U.S.A.* **93**, 9253 (1996).
16. M. E. Martone, V. M. Edelman, M. H. Ellisman, P. Nef, *Cell Tissue Res.* **295**, 395 (1999).
17. S. Sage, S. Ventéo, A. Jeromin, J. Roder, C. J. Dechesne, *Hearing Res.* **150**, 70 (2000).
18. M. Paterlini, V. Revilla, A. L. Grant, W. Wisden, *Neuroscience* **99**, 205 (2000).
19. R. Rivosecchi, O. Pongs, T. Theli, A. Mallart, *J. Physiol.* **474**, 223 (1994).
20. Supplemental information is available at Science Online (www.sciencemag.org/cgi/content/full/295/5563/2276/DC1).

21. H. Taschenberger, H. von Gersdorff, *J. Neurosci.* **20**, 9162 (2000).
22. Y. Kajikawa, N. Saitoh, T. Takahashi, *Proc. Natl. Acad. Sci. U.S.A.* **98**, 8054 (2001).
23. S. Iwasaki, T. Takahashi, *J. Physiol.* **509**, 419 (1998).
24. C. D. DeMaria, T. W. Soong, B. A. Alseikhan, R. S. Alvania, D. T. Yue, *Nature* **411**, 484 (2001).
25. T. Sakaba, E. Neher, *Neuron* **32**, 1119 (2001).
26. C.-Y. Wang et al., *Neuron* **32**, 99 (2001).
27. F. Helmchen, J. G. G. Borst, B. Sakmann, *Biophys. J.* **72**, 1458 (1997).
28. O. D. Uchitel et al., *Proc. Natl. Acad. Sci. U.S.A.* **89**, 3330 (1992).
29. T. Takahashi, A. Momiyama, *Nature* **366**, 156 (1993).
30. S. Iwasaki, A. Momiyama, O. D. Uchitel, T. Takahashi, *J. Neurosci.* **20**, 59 (2000).
31. Y. Tang, T. Schlumpberger, T. Kim, M. Lueker, R. S. Zucker, *Biophys. J.* **78**, 2735 (2000).
32. Supported by a grant-in-aid for scientific research from the Ministry of Education, Culture, Sports, Science and Technology of Japan, a research grant from the Mitsubishi Foundation (T.T.), and the Medical Research Council of Canada (A.J., J.C.R.).

21 November 2001; accepted 14 February 2002

The Medial Frontal Cortex and the Rapid Processing of Monetary Gains and Losses

William J. Gehring* and Adrian R. Willoughby

We report the observation of neural processing that occurs within 265 milliseconds after outcome stimuli that inform human participants about gains and losses in a gambling task. A negative-polarity event-related brain potential, probably generated by a medial-frontal region in or near the anterior cingulate cortex, was greater in amplitude when a participant's choice between two alternatives resulted in a loss than when it resulted in a gain. The sensitivity to losses was not simply a reflection of detecting an error; gains did not elicit the medial-frontal activity when the alternative choice would have yielded a greater gain, and losses elicited the activity even when the alternative choice would have yielded a greater loss. Choices made after losses were riskier and were associated with greater loss-related activity than choices made after gains. It follows that medial-frontal computations may contribute to mental states that participate in higher level decisions, including economic choices.

An important objective of our experimental design was to separate processing related to monetary gains and losses from other possible confounding factors. Our analyses compared results from conditions under which the physical characteristics of the stimuli were equivalent, ruling out the possibility that effects arose from processing related to physical differences between the stimuli. Moreover, the probabilities of the outcomes were equivalent, making the statistical expected value of the monetary outcome zero on each trial and ruling out potential confounding influences with the differential probability of a gain or loss (8).

Twelve participants (six males and six females, ranging in age from 19 to 30 years old) completed 768 trials of this gambling task while the electroencephalogram (EEG) was recorded from 42 scalp electrodes (9). The experimental session for each participant was divided into 24 blocks of 32 trials, and cumulative monetary awards were given at the end of each block (10). ERPs were computed by averaging the EEG records associated with each type of outcome stimulus (11).

Figure 2 compares the ERPs from gain trials and loss trials. It shows a negative-polarity ERP, beginning at about 200 ms after the outcome stimulus. The potential was larger on loss trials than on gain trials ($P = 0.0098$). As shown by the topographic map of scalp electrical activity in Fig. 2, the potential was largest at the medial-frontal scalp location Fz, ($P = 0.00022$) (9). We used dipole modeling to identify which cortical region was most likely to generate the pattern of loss-related electrical activity observed at the scalp. The results of the modeling were consistent with a source in the medial frontal cortex, in or near the anterior cingulate cortex (ACC) (Fig. 2) (9, 12). For convenience, we

A fighter pilot monitoring cockpit indicators, a stock-exchange trader checking prices, and a gambler playing blackjack in a casino all evaluate quickly whether events are good or bad and make rapid decisions on the basis of those events. Recent research indicates that such evaluations can take place quickly, automatically, and without conscious deliberation (1–3). In addition, there is growing knowledge about the neural systems that mediate such processing, in particular those concerned with reward and punishment (4–7). Yet there is still little direct evidence for neural processing in humans that is not only

fast enough to reflect this evaluation but also is directly related to choice behavior.

Here, we report the observation of neurophysiological activity with characteristics that are consistent with its involvement in rapidly evaluating the motivational impact of events and in guiding choice behavior. The activity responds to the monetary outcome signified by an event, operates on a short time scale, and covaries with the riskiness of people's choices in a gambling task. To investigate evaluative neural activity, we recorded event-related brain potentials (ERPs) from human participants as they performed a monetary gambling task (Fig. 1). Participants' choices were followed by outcome events signifying both the monetary gain or loss that resulted from their choice and the gain or loss that would have resulted from making the other choice.

Department of Psychology, University of Michigan, 525 East University, Ann Arbor, MI 48109–1109, USA.

*To whom correspondence should be addressed. E-mail: wgehring@umich.edu